Nonlinear vibrations of shape-morphing cantilever plates: modeling and analysis ⋆

Burak Gulsacan * **David Reiner** * **Cory Murphy** *
Matteo Aureli *,1

* *University of Nevada, Reno*
1664 N. Virginia St., Reno, NV 89557, USA

Abstract: We investigate the nonlinear vibration behavior of a shape-morphing cantilever plate excited by base acceleration and shape-morphing deformation, imposed by a periodic moment on the sides of the plate. The interplay of shape-morphing and base excitation causes the system to demonstrate distinctive and tunable nonlinear behavior. We present frequency responses based on a finite element parametric study of the actuation parameters, and propose a minimal modeling of the system based on the Duffing oscillator. This modeling is related to the physical actuation for analysis of nonlinear curvature-based tunable systems and could be used in future design scenarios.

Keywords: modeling, nonlinear plate vibrations, Duffing oscillator, variable stiffness, shape-morphing, Gaussian curvature

1. INTRODUCTION

The study of nonlinear vibrations and dynamics of cantilever beams and plates has played a key role in scientific and technical advancements for applications including atomic force microscopy (AFM), (micro)electromechanical systems for sensing, actuation, and energy harvesting, and biomimetic underwater propulsion (Leadenham and Erturk, 2014; Bajaj et al., 2016; Jackson and Gutschmidt, 2018; Yabuno, 2021). A fundamental source of nonlinearity lies in the effect of large displacements in certain vibration scenarios. Of particular interest are geometric nonlinearities, which arise when large deformations induce a nonlinear relationship between strain and curvature, thereby altering the structure's effective stiffness. In these cases, it is well known that the nonlinear effects become prominent and result in complex dynamic behavior in the system (Volmir, 1974; Soedel, 1993).

Despite this being an active research topic with still somewhat incomplete understanding (McHugh, 2020), the fundamental idea can be connected back to Theorema Egregium by Gauss, see Gauss (1902). Therein, it is stated that the Gaussian curvature of a surface, defined as the product of the two principal curvatures of the surface, remains invariant under local isometry. Based on this concept, several works have discussed curvature-induced stiffening of plates. For example, Shihab et al. (2021) have introduced an innovative approach to tuning the stiffness and natural frequencies of microplate sensors through an applied constant transverse curvature. The study demonstrated that transverse curvature effectively alters the static stiffness and natural frequencies of a microplate sensor. In dynamic conditions, curvature-based stiffening appears in fluid-structure interaction (FSI) scenarios as the so-called "shape-morphing" strategy introduced in Ahsan and Aureli (2017, 2018), where a time-varying curvature is applied in the chord direction of the plate. These studies suggest that shape-morphing can improve the maneuverability and efficiency of underwater vehicles by allowing for modulated force reduction through shape-morphing or increased thrust generation. While these works provide valuable insights into FSI applications of shape-morphing plates, the implications on the structural dynamics of the control architecture were not addressed therein. Thus, a knowledge gap still remains in understanding the detailed structural dynamics at play, especially with the addition of geometric nonlinearity via shape-morphing and its interplay with the transverse vibrations.

Motivated by these studies, as well as by preliminary experimental results on vibrations of shape-morphing plates actuated by smart materials and/or tendons, we seek to understand the structure-control interactions of shape-morphing plates vibrating in-vacuo. Therefore, in this paper, we investigate the concept of dynamic tunability of cantilever plate systems, specifically focusing on the nonlinear effects promoted by dynamically applied transverse curvature in the presence of large amplitude vibrations. Our prototype problem consists of a cantilever plate undergoing shape-morphing produced by distributed bending moments along the free edges of the plate. The moments are time-varying, and their magnitude is prescribed to be proportional to the deflection of the midline of the plate. This particular scenario can be effectively interpreted as a nonlocal boundary condition for the plate system.

We first perform a comprehensive parametric finite element analysis (FEA) of shape-morphing plates under base excitation to investigate their frequency response functions (FRFs) under different forcing and shape-morphing intensity. We elucidate the interplay of actuation parameters

⋆ This material is based in part on work supported by the National Science Foundation under Grant No. 1847513.
[1] Corresponding author. E-mail: maureli@unr.edu

and reveal landmarks of nonlinearity in our system, including frequency shifts, hardening and softening effects, amplitude jumps and hysteresis phenomena. By distilling the essential drivers of the observed nonlinear behavior, we then hypothesize that a forced Duffing oscillator (Nayfeh and Mook, 1979) can serve as an efficient minimal model for the dynamics of the system. To verify this hypothesis, we construct a parameter estimator based on the computational results that produces suitable governing parameters for an equivalent Duffing oscillator which replicates the complex nonlinear dynamics of the shape-morphing plate vibrating in-vacuo. This model hinges on the powerful theoretical results for the Duffing oscillator to provide a convenient framework for analysis of the physical system, bypassing the need of costly computational studies or rigorous theoretical treatment, which become prohibitive in real-time control applications.

The rest of this paper is organized as follows. In Section 2, we introduce the modeling approach for our prototype problem and describe the details of the FEA study. We demonstrate the distinctive nonlinearity of the system through a representative FRF and the effect of the physical parameters of the problem. In Section 3, we introduce the equivalent Duffing oscillator, propose a parameter estimation framework, and discuss the advantages of the minimal model for the purpose of analysis. Finally, conclusions are reported in Section 4.

2. COMPUTATIONAL MODELING

2.1 Problem statement

We consider a thin cantilever plate undergoing base excitation in vacuo, see Fig. 1(a). The plate is positioned within a Cartesian reference frame where the axis, width, and thickness of the plate lie along the x, y, and z-axes of the reference frame, respectively. The time variable is indicated by t. The origin of the reference frame is chosen to coincide with the centroid of the fixed end. The length, width, and thickness of the plate are denoted as L, b, and h, respectively. The material of the plate is linear elastic, homogeneous, and isotropic. The plate deflection field is indicated with $\tilde{w}(x, y, t)$.

To study the properties of structure-control interactions, we consider the effect of shape-morphing actuation provided to the plate by externally applied edge moments that arise in response to the plate gross deflection. The edge moments, distributed along the x-direction, are thus defined as $\tilde{M}(x,t) = \tilde{\kappa}_m \tilde{w}(x,0,t)$, see Fig. 1(a). Here, $\tilde{M}(x,t)$ represents a bending moment per unit length and has units of Nm/m, $\tilde{w}(x,0,t)$ is the deflection of the points along the mid-line of the plate, with units of m, and $\tilde{\kappa}_m$ is a moment coefficient which determines the proportionality of the applied moment with respect to the deflection of the points, along the mid-line of the plate and it has units of N/m. We define the coefficient $\tilde{\kappa}_m$ to be greater than 0 if it produces a negative Gaussian curvature on the surface during shape-morphing actuation, as shown in Fig. 1(c). Vice versa, $\kappa_m = 0$ in Fig. 1(b) corresponds to no shape-morphing actuation.

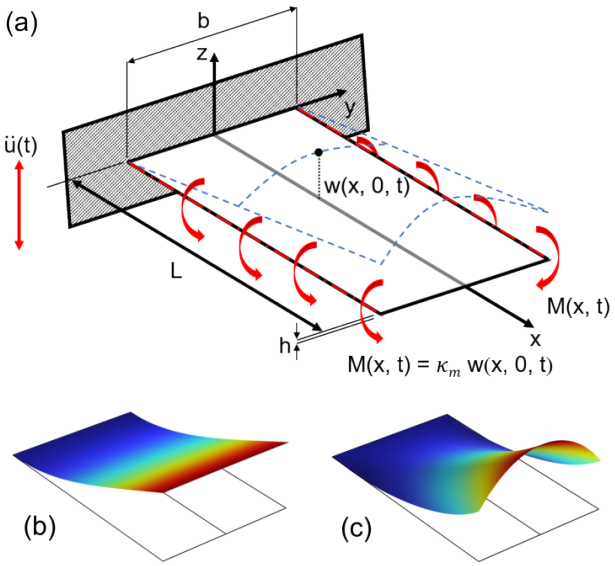

Fig. 1. In (a): Schematics and nomenclature of the problem. The plate is excited with a base acceleration and edge moments proportional to the displacement of the plate mid-line. In (b): Example of deflection under base excitation with no shape-morphing ($\kappa_m = 0$). In (c): Example of deflection under base excitation with shape-morphing, with positive moment coefficient ($\kappa_m > 0$).

2.2 Finite element analysis considerations

In this work, we perform a comprehensive finite element analysis study in COMSOL Multiphysics 6.0. Within the software, we then model a representative system whose geometric and material properties mimic closely those of an experimental testbed we also constructed for fluid-structure-control interaction studies. The plate has a length $L = 250\,\text{mm}$, width $b = 152.4\,\text{mm}$, and thickness $h = 0.1778\,\text{mm}$. The material (steel) properties include a Young's modulus $E = 200\,\text{GPa}$, density $\rho = 7850\,\text{kg/m}^3$, and Poisson's ratio $\nu = 0.3$.

The motion of the plate is prescribed by the superposition of two different actuation protocols, namely a harmonic base excitation along the z-axis and the chord-wise shape-morphing about the x-axis. The base excitation is provided with the `Gravity` function in the software, by defining a harmonic dimensional acceleration $\ddot{\tilde{u}} = \tilde{A}\sin(\omega t)$ to the system. Here, $\tilde{A}$ is the dimensional amplitude of the base acceleration and ω is the excitation frequency. The shape-morphing is provided through the linear extrusion function provided by the software. In detail, during the oscillation of the plate, the linear extrusion function measures the deflection of the points along the mid-line of the plate, as indicated in Fig. 1. Then, the function uses these deflection values as a simultaneous input to the moment to be exerted on the sides of the plate, to realize a nonlocal boundary condition.

To identify universal relationships among the parameters, we nondimensionalize all lengths and displacements with the characteristic length L of the plate, and all time scales with Ω_0, defined as the radian undamped natural fundamental frequency of the plate, under linear elastic

Table 1. Mesh convergence study.

Minimum cell size (μm)	Total degree of freedoms	Diff. (%)
50	40950	-
375	14430	1.37
1000	6150	1.90
2500	3366	2.51
4500	2550	2.51

conditions and in the absence of shape-morphing. For our aspect ratio $b/L \approx 0.61$, and for our materials choice, this frequency is determined from the FEA simulation as $\Omega_0 = (2\pi)2.3854\,\text{rad/s}$. With these definitions, the nondimensional plate deflection becomes $w = \tilde{w}/L$ and the nondimensional base excitation amplitude becomes $A = \tilde{A}/(\Omega_0^2 L)$. Furthermore, defining the plate bending stiffness $D = Eh^3/12(1-\nu^2)$, see Leissa (1969), the nondimensional nonlocal boundary condition becomes

$$M(x,t) = \kappa_m w(x,0,t) \tag{1}$$

where $\kappa_m = \tilde{\kappa}_m(L^2/D)$ is the nondimensional moment coefficient.

Transient, geometrically nonlinear, simulations are run on the system over several cycles of oscillations, long enough to ensure a steady-state response of the plate. To reconstruct a FRF of the primary resonances of the system, the excitation frequency is varied over a band comprising the first peak of the FRF, using a frequency increment of $0.1/\Omega_0$ to achieve a detailed representation of the response across the frequency spectrum. The response of the system is then extracted using spectral analysis (via Fast Fourier Transform) on the time history of the plate deflection sampled at $x = L$, $y = 0$.

We use the `Shell` module of COMSOL Multiphysics to reduce the computational cost and complexity of the simulations. The plate is modeled as a mathematical surface and mapped meshing is used. A convergence study is performed to assess the independence of results on the mesh size. In Table 1, we present the sensitivity of our FEA results to the mesh sizes for the most severe conditions of this study, that is, on of the largest input acceleration amplitudes $A = 0.0089$ and moment coefficients $\kappa_m = 5.46$, at the peak frequency $\omega/\Omega_0 = 1.51$. In the "Diff." column, we report deviations in percentage from the values determined with the mesh with minimum cell size equal to $50\,\mu$m. As all meshes are seen to provide results within 3%, the final mesh selected has a minimum cell size of $4500\,\mu$m.

Time stepping is automatically taken care by the software package to satisfy error bound criteria. For further postprocessing, we select a time resolution of 0.02 s at which the output deflection are made available to the user. This choice makes available approximately 20 samples per oscillation period.

Finally, to prevent undesired numerical issues at resonance, Rayleigh damping is used. The Rayleigh's coefficients are selected to provide approximately 10% damping ratio in the band between 1 and 3 Hz.

2.3 Results and discussions

In this section, we investigate a representative FRF of the shape-morphing plate at the nondimensional acceleration amplitude $A = 1.78 \times 10^{-4}$. This amplitude is chosen among many to demonstrate a complete nonlinear behavior of the system including frequency shifts, hardening and softening effects, amplitude jumps and hysteresis phenomena. Simulations for a single amplitude and moment coefficient are performed by a parametric sweep of the excitation frequency, from low to high values. To investigate possible hysteresis phenomena, the sweep is performed also in the reverse direction (Nayfeh and Mook, 1979).

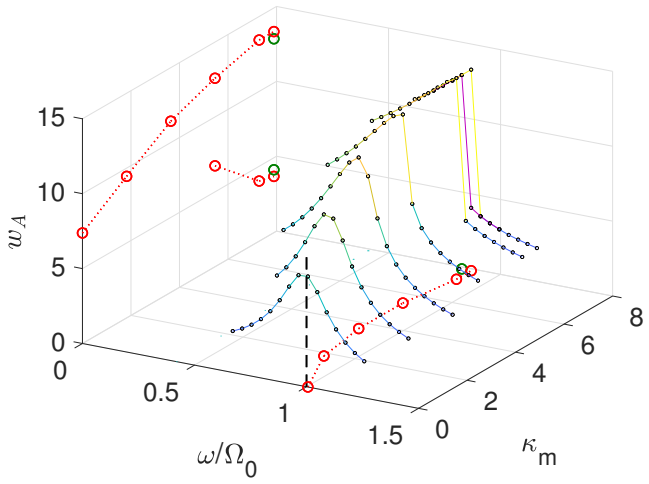

Fig. 2. FRF of the scaled plate tip deflection for various moment coefficients κ_m for the acceleration amplitude $A = 1.78 \times 10^{-4}$. The dashed line indicates the first eigenfrequency of the plate, $\omega/\Omega_0 = 1$.

To provide a more comprehensive understanding of the system behavior, the FRF below is displayed in terms of the nondimensional amplitude w_A. Specifically, this quantity is calculated from the amplitude of the steady state response $\tilde{w}(L,0,t)$ nondimensionalized as $w_A = \max_t \Omega_0^2|\tilde{w}(L,0,t)|/\tilde{A} = \max_t |\tilde{w}(L,0,t)/L|/A$. The FRFs are depicted in 3D plots, as a function of the nondimensional excitation frequency ω/Ω_0 and the moment coefficient κ_m, for each of the studied excitation amplitudes. In addition, the color scale in the FRF represent high and low values of the amplitudes. For further clarity, the peak values of the nondimensional amplitude and of the frequency are projected on the amplitude–moment coefficient and frequency–moment coefficient planes, so that the nonlinear behavior of the system is better visualized.

Figure 2 displays the FRF of the plate excited at $A = 1.78 \times 10^{-4}$ for various moment coefficients. At $\kappa_m = 0$, the plate is only excited with base acceleration without any prescribed shape-morphing. The FRF shows a resonance peak at $\omega/\Omega_0 = 1$ (by definition), with nondimensional amplitude $w_A = 7.38$. An increase of κ_m to 1.82, results in amplitude increase to $w_A = 9.45$ with simultaneous decrease in the peak frequency to $\omega/\Omega_0 = 0.88$, demonstrating a shape-morphing induced softening behavior for the plate. This phenomenon can be explained by observing that, in this case, vibration amplitudes are so small that they cannot elicit a strong hardening response due to geometric nonlinearities. The applied moments, on the other hand, tend to increase the plate displacements, with overall softening effect. For $\kappa_m = 3.64$, we observe the same qualitative softening behavior, as the nondimensional am-

plitude increases to 11.42 and the peak frequency decreases to 0.84. For $\kappa_m = 5.46$, the behavior of the FRF changes qualitatively, as a jump phenomenon can be observed from a larger value $w_A = 12.59$ to a smaller value $w_A = 6.73$, at a critical frequency $\omega/\Omega_0 = 0.84$. The general configuration of the FRF curve, for larger moment coefficients, is therefore that of a hardening system. The behavior can be explained by appealing to the nonlinear geometric effects that become more prominent at relatively large amplitudes and higher shape-morphing intensities. Interestingly, for the largest $\kappa_m = 7.89$ case, we observe the presence of hysteresis (Nayfeh and Mook, 1979), demonstrated by the multi-valued nature of the amplitude as a function of the excitation frequency. Specifically, the two branches of the FRF curve can be determined by separate frequency sweeps for increasing and decreasing values. In this case, the peak frequency occurs at $\omega/\Omega_0 = 0.88$ and $w_A = 13.42$ for increasing frequency sweep and at $\omega/\Omega_0 = 0.84$ and $w_A = 12.94$ for decreasing frequency sweep. For clarity, the jump pertaining to the decreasing sweep is indicated with a magenta line. Thus, Fig. 2 clearly diplays that the surface w_A as a function of ω/Ω_0 and κ_m is a cusp, see also Nayfeh and Mook (1979).

To better track the jump phenomena, we also project the amplitudes and frequencies in proximity of the jumps on the coordinate planes, indicated with red markers and lines. We observe that as κ_m increases, the jump phenomenon occurs at progressively increasing frequencies and its amplitude becomes progressively larger. For the largest moment coefficient $\kappa_m = 7.89$, we have also indicated with dark green markers the corresponding jumps associated to decreasing frequency sweep.

The study above illustrates that a variety of interesting, and sometimes contrasting, nonlinear dynamics effects can be elicited by proper actuation of the plate and via the structure-control interaction paradigm produced by shape-morphing. However, due to the complexity of the system, and to the computational cost of exploring these behaviors, it is difficult to design a proper actuation strategy that would yield a desired dynamic behavior, especially in view of real-time control applications. Therefore, in order to elucidate this complex link, we take a different approach and seek to pinpoint the main defining features of the system based on the observations from our computational campaign. To this aim, in Fig. 3, we specifically investigate the fundamental role of geometric nonlinearities and shape-morphing actuation on the response of the system, for relatively large excitation amplitude. In the computational framework, we can explicitly turn "on" or "off" either of these effects. Figure 3 displays two representative cases with different shape-morphing actuation described by the values $\kappa_m = 0$ and $\kappa_m = 3.64$. Both cases are solved using alternatively the nonlinear solver and a linear solver, for which the geometric nonlinearities are suppressed.

Without shape-morphing, for $\kappa_m = 0$, the inclusion of geometric nonlinearity stiffens the system, leading to a lower response amplitude. Notably, the peak frequency remains around $\omega/\Omega_0 = 1$ both linear and nonlinear cases. In the presence of shape-morphing, for $\kappa_m = 3.64$, a more dramatic effect is observed. The shape-morphing plate softens when geometric nonlinearity is not included in the solver. The peak frequency decreases to 0.76 for the linear

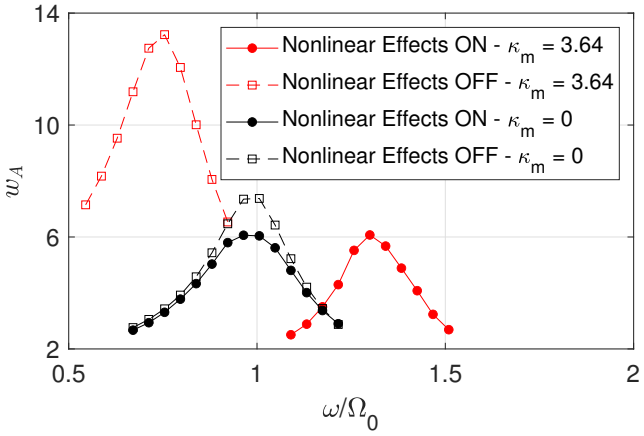

Fig. 3. Effect of geometric nonlinearity and shape-morphing on the response of the system for very large acceleration $A = 1.78 \times 10^{-2}$.

case, which also exhibits the highest amplitude among all scenarios. In contrast, the peak frequency for the nonlinear case shifts to a higher value of 1.3.

These results suggest that the essential nonlinear behavior of the system can be understood by using a minimal equation of motion, for example of the form $\ddot{q} + (1 - s_m + aq^2)q = -\ddot{u}$. Here, u and q are the nondimensional input and relative response of the system, respectively, and we have neglected damping for simplicity. Importantly, a is the nonlinearity coefficient of a supposed cubic nonlinearity, and s_m is the softening effect (assumed linear) due to shape-morphing. This minimal theoretical framework offers the capability to capture the behavior observed in the computational modeling of the shape morphing, at a highly reduced computational cost. The cubic nonlinearity can however be justified by postulating a one-mode solution to the equations of motion from the nonlinear plate theory of Tang et al. (2014), where cubic terms represent the dominant nonlinear effects, at least for small excitations.

This observation allows us to hypothesize that we can model our physical system with base excitation and shape-morphing through an equivalent forced Duffing oscillator (Nayfeh and Mook, 1979), endowed with damping and cubic nonlinearity. Because of the well developed theory on the forced Duffing oscillator, we aim at constructing an equivalent oscillator as a powerful tool for much simplified analysis and design for our physical system. This construction is detailed in Sec. 3.

3. AN EQUIVALENT DUFFING OSCILLATOR

3.1 Review of general theory

In this section, we introduce our minimal model for the shape-morphing plate based on the forced Duffing oscillator. In particular, we develop a framework for parameter estimation for an equivalent oscillator that recovers the dynamic behaviors observed in FEA studies.

The minimal equation capturing the softening and hardening behavior seen in the FEA study can be recast in terms of a forced Duffing oscillator, with a nonlinear cubic

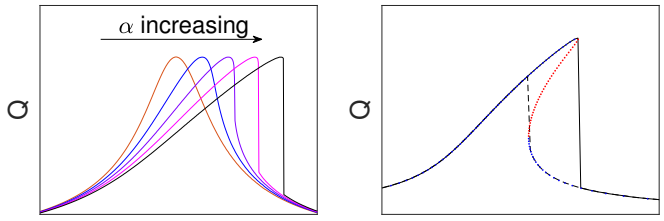

Fig. 4. In (a): Qualitative effect of the nonlinearity coefficient α in the Duffing equation on the system's response (nonlinear hardening in this case). In (b): Representative case of jump phenomena during increasing and decreasing frequency sweeps.

spring and damping, harmonically excited, whose governing equation reads (Nayfeh and Mook, 1979)

$$\ddot{q}(t) + 2\epsilon\mu\dot{q}(t) + \lambda^2 q(t) + \epsilon\alpha q(t)^3 = \epsilon U_0 \cos\omega t \qquad (2)$$

where $q(t)$ is the degree of freedom, λ is the natural undamped frequency of the linearized system, α is the nonlinearity coefficient of the cubic spring, U_0 is the nondimensional amplitude of the harmonic base excitation, occurring at a frequency ω, and μ is a viscous damping coefficient. In Eq. (2), ϵ is a small parameter that is conveniently introduced to develop a perturbation solution for the case of a weakly damped, weakly nonlinear system excited by a small amplitude harmonic term. Note that if $\epsilon \to 0$, the equation reduces to that of a harmonic oscillator.

Preliminary numerical analysis, shown in Fig. 4(a) via direct integration of Eq. (2) demonstrates the well-known effect of the nonlinearity coefficient α on the response of the system. As $\alpha > 0$ increases, the nonlinear spring is hardening and the FRF of the system, displaying the amplitude Q of the steady state vibration, bends towards higher frequencies. The FRFs in Fig. 4(a) are obtained by varying the frequency ω from low to high values. For relatively large values of α, the system exhibits amplitude jumps. This behavior is qualitatively consistent with the findings from our FEA study and motivates our search for an equivalent Duffing oscillator to capture the dynamics of our shape-morphing plate.

Further insight in the jump phenomena and in the overall FRF behavior of the forced Duffing oscillator can be obtained by a perturbation analysis of Eq. (2). Briefly, the frequency-amplitude relationship can be written in implicit form as (Nayfeh and Mook, 1979)

$$\omega = \lambda + \epsilon \left[\frac{3\alpha}{8\lambda} Q^2 \pm \sqrt{\frac{U_0^2}{4\lambda^2 Q^2} - \mu^2} \right] \qquad (3)$$

Because Q is a multi-valued function of ω, whereby multiple amplitude solutions coexist for a single frequency, it is known that the frequency-amplitude curve may exhibit a hysteresis phenomenon. The complete FRF demonstrating hysteresis, as shown in Fig. 4(b), can be constructed by calculating the resulting values for ω for suitable amplitudes Q. Two branches of the curve can be identified from Eq. (3), stemming from the $\pm$ sign in front of the radicand of Eq. (3). In Fig. 4(b), the analytical results from Eq. (3) are marked as dots, and are superimposed to lines from the numerical solution of Eq. (2). Note in particular that the dashed line corresponds to solutions for a decreasing frequency sweep from large to small frequencies. Finally, in Fig. 4(b) the blue dots correspond to stable branches in the solution, while the red dots indicate an unstable solution that cannot be produced by direct numerical integration of Eq. (2), see also Nayfeh and Mook (1979).

The analysis so far reveals four key parameters that govern the dynamic behavior of the forced Duffing oscillator: the nonlinearity coefficient α, the forcing amplitude U_0, the viscous damping coefficient μ, and the primary resonance frequency λ. We observe that ϵ in Eqs. (2) and (3) should not be interpreted as an independent parameter as it could be incorporated in a rescaling of α, U_0, and μ. Next, we develop a framework for parameter identification that will associate to each pair of physical actuation parameters in the FEA study, that is, A and κ_m, the quadruple $\boldsymbol{p} = \{\lambda, \alpha, U_0, \mu\}$ of parameters of the equivalent oscillator.

3.2 Parameter identification

Here, we employ an optimization technique which takes as an input the nondimensional amplitude w_A from the FEA study and performs a least squares calculation to estimate the parameters $\boldsymbol{p}$ of the equivalent Duffing oscillator. First, we use Eq. (3) to calculate the frequency ω when each data point for w_A is substituted for Q. In all calculations, we arbitrarily set the small parameter ϵ to 0.1, as it multiplies all terms with μ, α and U_0 in Eq. (2). Care should be taken to isolate the $\pm$ branches in Eq. (3). For example, focusing on the solution with the minus sign, we could rewrite Eq. (3) as $\omega^- = F^-(w_A^-, \boldsymbol{p})$ to emphasize the relationship among the frequency, amplitude, and Duffing parameters on the negative branch; a similar convention is adopted for the positive branch. Then, we compare this estimated frequency with the corresponding actual frequency values ω/Ω_0 from the FEA study. The discrepancy between the two is incorporated in the following sum-of-squared error function

$$E_{P2D}(\boldsymbol{p}) = \sum_{i=1}^{N^-} [F^-(w_{A,i}^-, \boldsymbol{p}) - \omega_i^-/\Omega_0]^2 + \sum_{i=1}^{N^+} [F^+(w_{A,i}^+, \boldsymbol{p}) - \omega_i^+/\Omega_0]^2 \qquad (4)$$

where the index i indicates datapoints from the FEA simulations and N^+ and N^- indicate the number of available datapoints on the positive and negative branches. Here the subscript $P2D$ indicates that the procedure converts the physical excitation parameters to the equivalent Duffing oscillator parameters. By minimizing Eq. (4) using the subroutine `fmincon` in MATLAB, we find the set of the four Duffing parameters (λ, α, U_0, and μ) that best fits the available data as argmin of $E_{P2D}(\boldsymbol{p})$.

To demonstrate the parameter identification framework, we show representative results for the nondimensional acceleration amplitude $A = 1.78 \times 10^{-4}$ in Fig. 5. Here, we display the FRFs of the FEA study for various moment coefficients indicated by different colors and full lines with empty markers. The specific values of κ_m are indicated for each curve. The curve fit by the equivalent Duffing oscillator is indicated with the dashed lines and the same corresponding color for each moment coefficient. The FEA

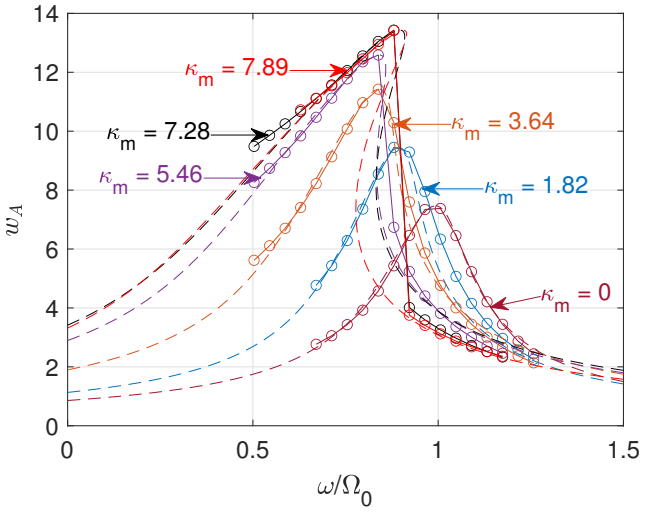

Fig. 5. FRFs of the equivalent Duffing oscillators superimposed on the nondimensional amplitude w_A obtained from the FEA study for various moment coefficients for the acceleration amplitude $A = 1.78 \times 10^{-4}$.

results and the curve fit by the Duffing oscillator show good agreement for all the cases, while slightly deteriorating for the more extreme cases of A and κ_m, where arguably the perturbation methods used to solve Eq. (2) are progressively less applicable. Additional sources of discrepancy may lie in the higher order nonlinearities of the plate behavior which are not incorporated in the Duffing equation. However, this qualitative agreement validates our parameter estimator strategy and the main hypothesis that the shape-morphing plate can be modeled with an equivalent forced Duffing oscillator.

4. CONCLUSIONS

In this study, we presented a framework for analysis of the structure-control interaction for a vibrating shape-morphing plate under base excitation. We have investigated the concept of dynamic curvature-based resonance and stiffness tuning for a prototype plate system via a detailed parametric finite element analysis study with particular focus on the distinctive nonlinear behavior of the system.

While computational modeling and nonlinear plate theories can in principle treat the complex nonlinear dynamics in these systems, we aimed at providing an understanding of the fundamental aspects of the nonlinear dynamics through a computationally manageable minimal model inspired by the behavior of the physical system. By carefully dissecting the interplay of geometric nonlinearity and shape-morphing actuation, we hypothesized that an equivalent forced Duffing oscillator can replicate and capture the essential features of our system. The hypothesis is verified through a parameter estimation framework that allows us to convert the physical actuation parameters to the governing parameters of an equivalent nonlinear oscillator.

We are currently extending the framework towards design applications, in which a desired dynamics (described by the minimal oscillator) can be enforced in the physical system via properly determined actuation parameters. Furthermore, we are conducting an experimental validation of our framework on a testbed including shape-morphing plates actuated by smart materials in both air and underwater environments, for applications including bioinspired underwater robotic propulsion. These results will be presented elsewhere.

REFERENCES

Ahsan, S.N. and Aureli, M. (2017). Nonlinear oscillations of shape-morphing submerged structures: Control of hydrodynamic forces and power dissipation via active flexibility. *Journal of Fluids and Structures*, 74, 35–52.

Ahsan, S.N. and Aureli, M. (2018). Three-dimensional analysis of hydrodynamic forces and power dissipation in shape-morphing cantilevers oscillating in viscous fluids. *International Journal of Mechanical Sciences*, 149, 436–451.

Bajaj, N., Sabater, A.B., Hickey, J.N., Chiu, G.T.C., and Rhoads, J.F.J. (2016). Design and implementation of a tunable, duffing-like electronic resonator via nonlinear feedback. *Journal of Microelectromechanical Systems*, 25(1), 2–10.

Gauss, K.F. (1902). *General investigations of curved surfaces of 1827 and 1825*. The Princeton University Library.

Jackson, S. and Gutschmidt, S. (2018). Utilization of a two-beam cantilever array for enhanced atomic force microscopy sensitivity. *Journal of Vibration and Acoustics*, 140(4).

Leadenham, S. and Erturk, A. (2014). Unified nonlinear electroelastic dynamics of a bimorph piezoelectric cantilever for energy harvesting, sensing, and actuation. *Nonlinear Dynamics*, 79(3), 1727–1743.

Leissa, A.W. (1969). *Vibration of plates*. Office of Technology Utilization, NASA, Washington, D.C.

McHugh, K.A. (2020). *Large Deflection Inextensible Beams and Plates and their Responses to Nonconservative Forces: Theory and Computations*. Ph.D. thesis, Duke University.

Nayfeh, A.H. and Mook, D.T. (1979). *Nonlinear Oscillations*. Wiley.

Shihab, R., Jalil, T., Gulsacan, B., Aureli, M., and Tung, R. (2021). Sensor egregium-an atomic force microscope sensor for continuously variable resonance amplification. *ASME Journal of Vibration and Acoustics*, 143(4), 041013.

Soedel, W. (1993). *Vibrations of Shells and Plates*. Marcel Dekker, New York, NY, 2 edition.

Tang, D., Zhao, M., and Dowell, E.H. (2014). Inextensible beam and plate theory: Computational analysis and comparison with experiment. *Journal of Applied Mechanics*, 81(6).

Volmir, A.N. (1974). The nonlinear dynamics of plates and shells. Technical Report AD-781 338, Foreign Technology Division Wright-Patterson Air Force Base, Ohio.

Yabuno, H. (2021). Review of applications of self-excited oscillations to highly sensitive vibrational sensors. *ZAMM - Journal of Applied Mathematics and Mechanics / Zeitschrift für Angewandte Mathematik und Mechanik*, 101(7), e201900009.